Uncertainty analysis in food engineering involving imprecision and randomness

Cédric Baudrit, Arnaud Helias, Nathalie Perrot

Uncertainty analysis in food engineering involving imprecision and randomness

Cédric Baudrit
cbaudrit@grignon.inra.fr

Arnaud Hélias
arnaud.helias@grignon.inra.fr

Nathalie Perrot
nathalie.perrot@grignon.inra.fr

UMR782 Génie et Microbiologie des Procédés Alimentaires
INRA, AgroParisTech
F-78850 Thiverval-Grignon, France

Abstract

During the cheese ripening, airflow pattern and climatic conditions inside cheese-ripening rooms are determinant for cheese weight losses. Due to the variation of air velocity inside ripening chambers, homogeneity in the distribution of climatic conditions is very hard to achieve at every single point of it. We are hence faced with imprecise and incomplete knowledge. In practice, it is common that some model parameters may be represented by single probability distributions, justified by substantial data, while others are more faithfully represented by possibility distributions due to the partial nature of available knowledge. This paper applies recent methods, designed for the joint propagation of variability and imprecision, to a cheese ripening mass loss model. Joint propagation methods provide lower & upper probability bounds of exceeding a certain value of cheese mass losses.

Keywords. Imprecise probabilities, p-boxes, belief functions, possibility, food processing, cheese ripening.

1 Introduction

In the food industry, end-products must achieve a compromise between several properties, including sensory, sanitary, technological properties. Among the latter, sensory and sanitary properties are essential because they influence consumer choice and preference. Nevertheless, managing these properties right from the fabrication stage with the aim of controlling them is no easy task ([23, 24]). One of the key reasons of this difficulty is the uncertainty that should be managed at different levels:

- Uncertainty (more specifically imprecision) on the measurements, especially the measurements of the sensory properties [15]. It is obvious and accepted that there is a lack of efficient sensors, and that existing sensors often provide incomplete information for taking action decisions on the process [17]. Moreover, when adequate sensors exist, the configurations of industrial processes do not often allow an efficient placement.

- Uncertainty on the phenomenon involved, even for control purposes. As a consequence the management of uncertainty on the parameters and also the structure of the models built are crucial [16].

Few contributions about this topic are available. Among them Davidson et al. [5] used a fuzzy arithmetic that estimates peanut eating time and browning to control peanut roasting. Perrot et al. [24] developed a decision help system to control the cheese ripening process, integrating the uncertainty of human measurements. Petermeier et al. [25] used a hybrid approach to develop a model of the fouling behavior of an arbitrary heat treatment device for milk. This is developed by combining deterministic differential equations with cognitive elements for the unknown parts of the knowledge model. These authors emphasize the relevance of this open field of research in the context of food processes and the interest of fuzzy symbolic representation of expert reasoning. Nevertheless, they call into question the optimality of the approaches developed on the basis of imperfect and incomplete expert knowledge.

The ripening process is one most important step for many cheese makers. Microbial activities, responsible for the organoleptic characteristics of cheeses, are influenced by climatic conditions (air temperature and relative humidity, gas concentration). So, controlling these climatic conditions inside cheese-ripening rooms is of paramount importance. Cheese mass loss dynamic is a key point in ripening process, with consequences on productivity and it introduces a risk that resulting product may be dropped in status (e.g., the Camembert-Normandie protected designation of origin requires a final weight of 0.25 kg).

Ventilation is used to evacuate heat and humidity generated by cheeses and the spatial distribution of climatic conditions inside cheese-ripening rooms is dependent on airflow (air velocity, air change rate). Nevertheless, only a few studies on interaction between climatic conditions and

airflow can be found in the literature due to confidentiality conditions. The distribution of climatic conditions is very hard to achieve at every single point of ripening chambers. In a industrial context, computational fluid dynamic model of ripening rooms [20] can not be carried out without an exhaustive room description. However, it is inconceivable to install sensors everywhere inside ripening chambers to pick up for instance temperature and relative humidity. Hence, we are faced with imprecise knowledge relative to the spatial variability of climatic conditions. Heat and mass transfert are a well studied phenomenon in cooking or drying process. However, little data have been published for the cheese ripening and transfert coefficients between cheese and atmosphere are not precisely described.

It is more and more acknowledged that uncertainty regarding model parameters has essentially two origins [12]. It may arise from randomness (often referred to as "stochastic uncertainty") due to natural variability of observations resulting from heterogeneity or the fluctuations of a quantity in time. Or it may be caused by imprecision (often referred to as "epistemic uncertainty") due to a lack of information. This lack of knowledge may stem from a partial lack of data, either this data is impossible to collect, or because only experts can provide some imprecise information. For example, it can be quite common for an expert to estimate numerical values of parameters in the form of confidence intervals according to his/her experience and intuition. The uncertainty pervading model parameters is not of a single nature, namely, randomness and incomplete knowledge may coexist, especially due to the presence of several, heterogeneous sources of knowledge, as for instance statistical data and expert opinions. The most general setting to recognize incompleteness as a feature distinct from randomness is the one of imprecise probabilities developed at length by Peter Walley [29]. In this theory, sets of probability distributions capture the notion of partial lack of probabilistic information. In practice, while information regarding variability is best conveyed using probability distributions, information regarding imprecision is more faithfully conveyed using families of probability distributions. Probability boxes [11] or possibility distributions (also called fuzzy intervals) [9] or yet belief function introduced by Dempster [7] (and elaborated further by Shafer [27] and Smets [28] in a different context) allow to encode such families. Most researchers typically use either one or the other of these modes of uncertainty representation [5, 23, 24, 25]. But to date, such combinations of these different modes of representation have never been applied to food processing.

In Section 2, we recall basic concepts of probability-boxes, numerical possibility theory and belief function in connection with imprecise probabilities. In Section 3, we present methods for propagating objective (variability) and subjective (imprecision) information through multivariate function. We also present post-processing to estimate confidence intervals and/or the probability of exceeding a threshold. In Section 4, we give an overview of a simplified cheese mass loss dynamic model with available knowledge associated to model inputs and their representation. Lastly, in Section 5, we process uncertainty on cheese mass loss model.

2 Concise representations of imprecise probability

Consider a probability space $(\Omega, \mathcal{A}, P)$. Let $\mathcal{P}$ be a probability family on the referential Ω and X be a random variable associated with probability measure P. In the following, we consider three frameworks for representing special sets of probability functions, which are more convenient for a practical handling.

2.1 Probability boxes

Suppose $\overline{F}_X$ and $\underline{F}_X$ are nondecreasing functions from the real line $\mathbb{R}$ into $[0, 1]$ such that $\underline{F}_X(x) \leq F_X(x) \leq \overline{F}_X(x)$, $\forall x \in \mathbb{R}$. The interval $[\underline{F}_X, \overline{F}_X]$ is called a "probability box" or "p-box" [11]. It encodes the class of probability measures whose cumulative distribution functions F_X are restricted by the bounding pair of cumulative distribution functions $\underline{F}_X$ and $\overline{F}_X$.
A p-box can be induced from the probability family $\mathcal{P}$ by $\forall x \in \mathbb{R}$:

$$\underline{F}(x) = \inf_{P \in \mathcal{P}} P((-\infty, x]); \ \overline{F}(x) = \sup_{P \in \mathcal{P}} P((-\infty, x]). \quad (1)$$

Let $\mathcal{P}(\underline{P} < \overline{P}) = \{P, \forall A \subseteq \Omega \text{ measurable}, \underline{P}(A) \leq P(A) \leq \overline{P}(A)\}$ be the probability family limited by upper $\overline{P}$ and lower $\underline{P}$ probabilities induced from $\mathcal{P}$. Clearly $\mathcal{P}$ is a proper subset of $\mathcal{P}(\underline{P} < \overline{P})$ generally. Let $\mathcal{P}(\underline{F}_X \leq \overline{F}_X)$ be the probability family containing $\mathcal{P}$ and defined by

$$\mathcal{P}(\underline{F}_X \leq \overline{F}_X) = \{P \in \mathcal{P}, \forall x \in \mathbb{R}, \underline{F}_X(x) \leq F(x) \leq \overline{F}_X(x)\}. \quad (2)$$

Generally $\mathcal{P}(\underline{F}_X \leq \overline{F}_X)$ strictly contains $\mathcal{P}(\underline{P} < \overline{P})$, hence also the set $\mathcal{P}$ it is built from. The probability box $[\underline{F}_X, \overline{F}_X]$ provides a bracketing of some ill-known cumulative distribution function and the gap between $\underline{F}_X$ and $\overline{F}_X$ reflects the incomplete nature of the knowledge, thus picturing the extent of what is ignored.

2.2 Numerical possibility theory

Possibility theory [9] is relevant to represent consonant imprecise knowledge. A possibility distribution can model imprecise information regarding a fixed unknown parameter and it can also serve as an approximate representation

of incomplete observation of a random variable. The basic notion is the possibility distribution, denoted π, describing the more or less plausible values of some uncertain variable X. Possibility theory provides two evaluations of the likelihood of an event: the possibility Π and the necessity N. The normalized measure of possibility Π (respectively necessity N) is defined from the possibility distribution π : $\mathbb{R} \rightarrow [0, 1]$ such that $\sup_{x \in \mathbb{R}} \pi(x) = 1$ as follows:

$$\Pi(A) = \sup_{x \in A} \pi(x), \, N(A) = 1 - \Pi(\overline{A}) = \inf_{x \notin A}(1 - \pi(x)). \quad (3)$$

Numerical possibility distribution may also be viewed as a nested set of confidence intervals, which are the α-cuts $[\underline{x}_\alpha, \overline{x}_\alpha] = \{x, \pi(x) \geq \alpha\}$ of π. The degree of certainty that $[\underline{x}_\alpha, \overline{x}_\alpha]$ contains X is $N([\underline{x}_\alpha, \overline{x}_\alpha])$ (= $1 - \alpha$ if π is continuous). Conversely, given a nested set of intervals A_i with degrees of certainty λ_i that A_i contains X is equivalent to the possibility distribution

$$\pi(x) = \min_{i=1...n} \{1 - \lambda_i, x \in A_i\}, \quad (4)$$

provided that λ_i is interpreted as a lower bound on $N(A_i)$, and π is chosen as the least specific possibility distribution satisfying these inequalities [10].

We can interpret any pair of dual functions necessity/possibility $[N, \Pi]$ as upper and lower probabilities induced from specific probability families.

- Let π be a possibility distribution inducing a pair of functions $[N, \Pi]$. We define the probability family $\mathcal{P}(\pi) = \{P, \forall A \text{ measurable}, N(A) \leq P(A)\} = \{P, \forall A \text{ measurable}, P(A) \leq \Pi(A)\}$. In this case, $\sup_{P \in \mathcal{P}(\pi)} P(A) = \Pi(A)$ and $\inf_{P \in \mathcal{P}(\pi)} P(A) = N(A)$ (see [6, 10]) hold. In other words, the family $\mathcal{P}(\pi)$ is entirely determined by the probability intervals it generates.

- Suppose pairs (interval A_i, necessity weight λ_i) supplied by an expert are interpreted as stating that the probability $P(A_i)$ is at least equal to λ_i where A_i is a measurable set. We define the probability family as follows: $\mathcal{P}(\pi) = \{P, \forall A_i, \lambda_i \leq P(A_i)\}$. We thus know that $\sup_{P \in \mathcal{P}(\pi)} P(A) = \Pi(A)$ and $\inf_{P \in \mathcal{P}(\pi)} P(A) = N(A)$ (see [10], and in the infinite case [6]).

We can define a particular p-box $[\underline{F}, \overline{F}]$ from the possibility distribution π such that $\underline{F}(x) = N((-\infty, x])$ and $\overline{F}(x) = \Pi((-\infty, x]) \, \forall x \in \mathbb{R}$. But this p-box contains many more probability functions than $\mathcal{P}(\pi)$ (see [1] for more details about comparative expressivity of p-box and possibility distribution).

2.3 Belief function induced from random sets

The theory of imprecise probabilities introduced by Dempster [7] (and elaborated further by Shafer [27] and

Smets [28] in a different context) allows imprecision and variability to be treated separately within a single framework. Indeed, it provides mathematical tools to process information which is at the same time of random and imprecise nature. A random set on Ω is defined by a mass assignment ν which is a probability distribution on the power set of Ω. We assume that ν assigns a positive mass only to a finite family of subsets of Ω called the set $\mathcal{F}$ of focal subsets. Generally $\nu(\emptyset) = 0$ and $\sum_{E \in \mathcal{F}} \nu(E) = 1$. A random set induces set functions called plausibility and belief measures respectively denoted by Pl and Bel, and defined by Shafer [27] as follows:

$$Bel(A) = \sum_{E, E \subseteq A} \nu(E), \, Pl(A) = \sum_{E, E \cap A \neq \emptyset} \nu(E). \quad (5)$$

$Bel(A)$ gathers the imprecise evidence that asserts A; $Pl(A)$ gathers the imprecise evidence that does not contradict A.

These set-functions can be interpreted as families of probability measures, even if this view does not match the original motivation of Shafer [27] and Smets [28] for belief functions. A mass distribution ν may encode the probability family $\mathcal{P}(\nu) = \{P \in \mathcal{P}/\forall A \subseteq \Omega, Bel(A) \leq P(A)\} = \{P \in \mathcal{P}/\forall A \subseteq \Omega, P(A) \leq Pl(A)\}$. This family generates lower and upper probability functions that coincide with the belief and plausibility functions, *i.e.*

$$Pl(A) = \sup_{P \in \mathcal{P}(\nu)} P(A), \quad Bel(A) = \inf_{P \in \mathcal{P}(\nu)} P(A) \quad (6)$$

Originally, Dempster [7] considered imprecise probabilities induced from a probability space via a set-valued mapping Γ from a probability space $(\Omega, \mathcal{A}, P)$ to S (yielding a random set). For simplicity assume $\forall \omega \in \Omega, \Gamma(\omega) \neq \emptyset$. Let $X : \Omega \rightarrow S$ be a random variable such that $\forall \omega \in \Omega, X(\omega) \in \Gamma(\omega)$ and P_X be its associated probability measure such that $P_X(A) = P(X^{-1}(A))$. Define upper and lower probabilities as follows:

$$\overline{P}(A) = \sup_{X \in S(\Gamma)} P_X(A) \quad \underline{P}(A) = \inf_{X \in S(\Gamma)} P_X(A) \quad (7)$$

where $S(\Gamma) = \{X : \Omega \rightarrow S | X(\omega) \in \Gamma(\omega), \forall \omega \in \Omega\}$. For all measurable subsets $A \subseteq \Omega$, we have $\underline{A} \subseteq A \subseteq \overline{A}$ where $\underline{A} = \{\omega \in \Omega / \Gamma(\omega) \subseteq A\}$ and $\overline{A} = \{\omega \in \Omega / \Gamma(\omega) \cap A \neq \emptyset\}$. By defining the mass distribution ν_Γ on Ω by $\nu(E) = P(\{\omega / \Gamma(\omega) = E\})$. We thus retrieve belief and plausibility functions as follows:

$$\underline{P}(A) = P(\underline{A}) = Bel_\Gamma(A) = \sum_{E \subseteq A} \nu_\Gamma(E) \quad (8)$$

$$\overline{P}(A) = P(\overline{A}) = Pl_\Gamma(A) = \sum_{E \cap A \neq \emptyset} \nu_\Gamma(E) \quad (9)$$

We may define an upper $\overline{F}$ and a lower $\underline{F}$ cumulative distribution function (a particular p-box) such that $\forall x \in \mathbb{R}$, $\underline{F}(x) \leq F(x) \leq \overline{F}(x)$ with :

$$\overline{F}(x) = Pl(X \in (-\infty, x]); \underline{F}(x) = Bel(X \in (-\infty, x]). \quad (10)$$

But this p-box contains many more probability functions than $\mathcal{P}(v)$.

2.4 Discretized encoding of probability, possibility and p-boxes a random sets

Belief functions [7, 27] encompass possibility, probability and probabiliy-boxes theories in the discrete case. Hence, we can encode probability distribution p, p-box $[\underline{F}_X, \overline{F}_X]$ and possibility distribution π by using mass distribution v. In the continuous case, the representation will be approximate in a discrete framework for being able to do computations.

1. Probability → Belief function.
   Let X be a real random variable. In the discrete case, focal elements are singletons $(\{x_i\})_i$ and the mass distribution v is defined by $v(\{x_i\}) = P(X = x_i)$. In the continuous case, we define focal intervals $((x_i, x_{i+1}])_i$ by discretizing probability density into m intervals and a mass distribution v is defined by $v((x_i, x_{i+1}]) = P(X \in (x_i, x_{i+1}])$, $\forall\, i = 1 \ldots m$.

2. Possibility → Belief function.
   Let X be a ill-known random variable described by a possibility distribution π. Focal sets correspond to the α-cuts

   $$\pi_{\alpha_j} = \{x | \pi(x) \geq \alpha_j\}, \ \forall\, j = 1...q$$

   of possibility distribution π associated with X such that $\alpha_1 = 1 \geq \alpha_j \geq \alpha_{j+1} \geq \alpha_q > 0$ and $\pi_{\alpha_j} \subseteq \pi_{\alpha_{j+1}}$. Mass distribution v is defined by $v(\pi_{\alpha_j}) = \alpha_j - \alpha_{j+1}$ $\forall\, j = 1 \ldots q$ where $\alpha_{q+1} = 0$.

3. P-box → Belief function.
   Let X be a ill-defined random variable represented by a p-box $[\underline{F}_X, \overline{F}_X]$. By putting

   $$\underline{F}_X^{-1}(p) = \min\{x | \underline{F}_X(x) \geq p\}, \ \forall\, p \in [0, 1] \qquad (11)$$

   $$\overline{F}_X^{-1}(p) = \min\{x | \overline{F}_X(x) \geq p\}, \ \forall\, p \in [0, 1] \qquad (12)$$

   we can choose focal sets of the form $([\overline{F}_X^{-1}(p_i), \underline{F}_X^{-1}(p_i)])_i$ and the mass distribution v such that $v([\overline{F}_X^{-1}(p_i), \underline{F}_X^{-1}(p_i)]) = p_i - p_{i-1}$ where $1 \geq p_i > p_{i-1} > 0$. In this case, Kriegler et al. [18] have showed that we have $\mathcal{P}(\underline{F}_X \leq \overline{F}_X) = \mathcal{P}(v)$.

3 Propagating general heterogeneous information

This section is dedicated to the combination and the propagation of three kinds of information: pure random variables, imprecisely known fixed quantities, and imprecise

random variables (see [2, 3] for more details about the joint propagation methods of variability and imprecision). $\overrightarrow{X} : \Omega \to \mathbb{R}^k$ is a random vector that is observed with total precision; $\overrightarrow{Y} = (y_1, \ldots, y_l)$ is a deterministic vector and we have partial information about it. Finally, $\overrightarrow{Z} : \Omega \to \mathbb{R}^n$ is a random vector observed with imprecision. In our model we suppose that there exists an unidimensional random variable, $T : \Omega \to \mathbb{R}$, that can be expressed of the form $T = f(\overrightarrow{X}, \overrightarrow{Y}, \overrightarrow{Z})$, where the mathematical model described by the function $f : \mathbb{R}^{k+l+n} \to \mathbb{R}$ is totally well-known. We will try to represent the information about the probability distribution of T based on the information available, about $\overrightarrow{X}$, $\overrightarrow{Y}$ and $\overrightarrow{Z}$, respectively.

First, as $\overrightarrow{X}$ is a random vector, it can be considered as a particular case of multidimensional random set (a singleton in $\mathbb{R}^k$). Thus, in our model, we can assume it as part of vector $\overrightarrow{Z}$.

To simplify the notation, suppose $\overrightarrow{Z} = (Z_1, Z_2)$ and $\overrightarrow{Y} = (y_1, y_2)$. The imprecise knowledge about y_1 (resp. y_2) is modeled by a possibility distribution π^1 (resp. π^2). Thus, with a confidence level $1 - \alpha$, the parameter y_1 (resp. y_2) belongs to α-cut $\pi_\alpha^1 = \{x \in \mathbb{R} \mid \pi^1(x) \geq \alpha\}$ (resp. $\pi_\alpha^2 = \{x \in \mathbb{R} \mid \pi^2(x) \geq \alpha\}$). Let us encode π^1 as belief function by their focal sets:

$$\pi_{\alpha_i}^1 = \{x \in \mathbb{R} \mid \pi^1(x) \geq \alpha_i\}, \forall i = 1 \ldots q \qquad (13)$$

such that $\pi_{\alpha_i}^1 \subseteq \pi_{\alpha_{i+1}}^1$ with respective masses $v_i^1 = v(\pi_{\alpha_i}^1) = \alpha_i - \alpha_{i+1}$, $\forall i = 1 \ldots q$ where $\alpha_1 = 1 \geq \alpha_i \geq \alpha_{i+1} \geq \alpha_q > 0$ and $\alpha_{q+1} = 0$. We proceed in the same way for π^2. Let $(C_j^1, m_j^1)_{j=1...r}$ (resp. $(C_l^2, m_l^2)_{l=1...r}$) be the focal sets and the mass distribution associated to Z_1 (resp. Z_2).

Now, we need to represent the available information about the probability measure P_T induced by T. The probability measure of T is imprecisely determined by means of the basic assignment (denoted v_{ijkl}^T), associated with the focal sets

$$T_{ijkl} = f(\pi_{\alpha_i}^1, \pi_{\alpha_j}^2, C_k^1, C_l^2)$$

of T by $\forall i, j, k, l$:

$$v_{ijkl}^T = P(Y_1 = \pi_{\alpha_i}^1, Y_2 = \pi_{\alpha_j}^2, Z_1 = C_k^1, Z_2 = C_l^2)$$

In practice, only the marginals of the joint mass assignment are known, because no assumption is made about the relationship between the observation processes. If, in particular, independence between focal sets is assumed, the mass distribution becomes:

$$\forall i, j, k, l \quad v_{ijkl}^T = v_i^1 \times v_j^2 \times m_k^1 \times m_l^2$$

Hence, if we want to estimate $Pl^T(A)$ for all measurable

set A, using the definition of v_{ijkl}^T, we have:

$$Pl^T(A) = \sum_{(i,j,k,l):A\cap T_{ijkl}\neq\emptyset} v_{ijkl}^T, \quad Bel^T(A) = \sum_{(i,j,k,l):T_{ijkl}\subseteq A} v_{ijkl}^T$$

It corresponds to applying a Monte-Carlo method to all variables. For each possibility distribution, an α-cut is independently selected. This approach is a conservative counterpart to the calculus of probabilistic variables under stochastic independence [4].

Suppose now the same value of α is selected in the Monte-Carlo simulation for y_1 and y_2. Then, $\forall i, j, k, l$:

$$\alpha_i = \alpha_j \quad v_{ijkl}^T = v_{\alpha_i}^{y_1,y_2} m_k^1 m_l^2$$
$$\alpha_i \neq \alpha_j \quad v_{ijkl}^T = 0$$

The joint possibility distribution π associated to (y_1, y_2) is characterized by $min(\pi^1, \pi^2)$ which corresponds to the nested cartesian products of α-cuts and $v_i^{y_1,y_2}$ is the mass associated to the Cartesian product $\pi_{\alpha_i}^1 \times \pi_{\alpha_i}^2$. The use of "minimum" assumes the non-interaction of y_1, y_2, which expresses a lack of knowledge about the links between the values of y_1, y_2 and a lack of commitment as to whether y_1, y_2 are linked or not. We thus assume a total dependence between focal elements associated to possibilistic variables. This suggests that, if the source informing on y_1 is rather precise, then the one informing on y_2 is also precise (for instance it is the same source). However, this form of dependence does not presuppose any genuine functional (objective) dependence between possibilistic variables inside the domain $\pi_\alpha^1 \times \pi_\alpha^2$ (observed phenomenons). Hence, if we want to estimate $Pl^T(A)$ and $Bel^T(A)$ using the last definition of v_{ijkl}^T, we deduce:

$$Pl^T(A) = \sum_{jk} \Pi_{jk}^T(A)\times m_k^1\times m_l^2, \quad Bel^T(A) = \sum_{jk} N_{jk}^T(A)\times m_k^1\times m_l^2$$

where Π_{jk}^T are the possibility measures associated with the joint non-interactive possibility distribution π_{jk}^T obtained by means of the extension principle [8]:

$$\pi_{jk}^T(t) = \sup_{\substack{(y_1,y_2)\in\mathbb{R}^2,\\(z_1,z_2)\in C_j^1\times C_k^2,\\f(y_1,y_2,z_1,z_2)=t}} min(\pi^1(y_1),\pi^2(y_2))$$

This technique thus computes the eventwise weighted average of the possibility measures associated with each output fuzzy interval, and applies to any event. It is easy to extend this propagation method for more than four variables.

4 Case description

Our example is concerned with the ripening of a soft mould cheese (camembert type). A model has been built

[14] to estimate the mass loss of a cheese during ripening according to the close atmosphere. Our aim is to estimate confidence intervals or probability that cheese weight exceeds a threshold during ripening by taking into account uncertainty relative to measures and model parameters.

4.1 The ripening chamber

Soft cheeses (Camembert type) were manufactured in a sterile environment as previously described [22]. After drainage, 45 cheeses were aseptically transferred to a sterile pilot ripening chamber (see Figure 1). The average weigh of cheese was 0.333 kg with a standard deviation of 0.023 kg.

The ripening chamber ($0.91m^3$) was placed into a refrigerated room to allow the temperature regulation (see Figure 1). A cheese was continuously weighted with an elec-
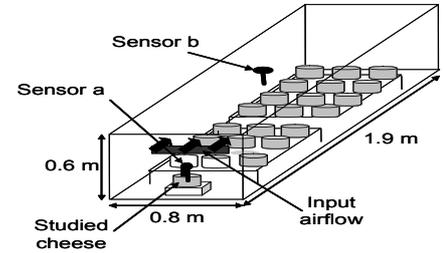
Figure 1: cheese-ripening room

tronic balance. Two combined sensors measured atmospheric temperature and relative humidity: 6 cm above the weighted cheese (see Figure 1, position a) and in the center of ripening chamber (see Figure 1, position b). Atmospheric changes were also characterized with CO_2 and O_2 sensors [26]. When the ripening chamber was used without input airflow, variations of these gas concentrations were depending only of cheese respiratory activity (CO_2 production and O_2 consumption). The ripening was performed with a periodically renewed atmosphere: if necessary, the CO_2 concentration was decreased to 2% by daily air injection with 6 m^3/h flow rate. In practical, the atmosphere was not renewed except 30 min per day. The ripening duration was 15 days, cheese were turned over on day 5. All online data were carried out with a 6 min acquisition period.

4.2 Model of Cheese mass loss

Cheese mass loss dynamic results from exchange between product (cheese) and close atmosphere. A schematic view of system is illustrated by Figure 2. Biological activities induce a matter flux between the cheeses and atmosphere of the ripening chamber: oxygen consumption and carbon dioxide release. r_{o_2}, the O_2 consumption, and r_{co_2}, the CO_2 production rates ($mol.m^{-2}.s^{-1}$) are obtained by deriving CO_2 and O_2 atmospheric concentrations. The respiration
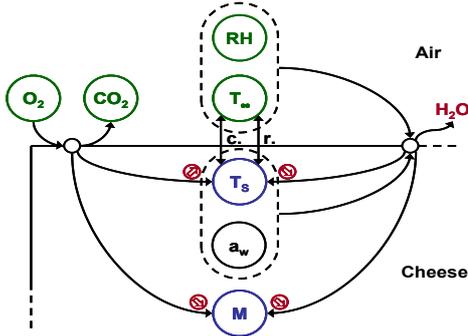
Figure 2: Schematic view of mass loss phenomenon.

matter flux ϕ_r (kg.m^{-2}.s^{-1}), is obtained by the difference between these two rates balanced by the molar masses

$$\phi_r = w_{o_2} r_{o_2} - w_{co_2} r_{co_2} \qquad (14)$$

with w_{o_2} and w_{co_2} the respective molar masses (kg.mol^{-1}). Because the O_2 consumption and CO_2 production rates have the same dynamic, the following simplification is used:

$$\phi_r \simeq (w_{o_2} - w_{co_2}) r = w_c r \qquad (15)$$

with

$$r = \left(\frac{r_{o_2} + r_{co_2}}{2} \right) \qquad (16)$$

The two rates are merged in r, corresponding to the respiratory activity. This simplification can be easily done because the carbon loss represents only 3% of the total mass loss.

The difference between water vapor pressure in the atmosphere and at the cheese surface causes an evaporative flux ϕ_w classically represented as following:

$$\phi_w = k \left(a_{ws} P_{sv}(T_s) - rh P_{sv}(T_\infty) \right) \qquad (17)$$

with a_{ws} the cheese surface water activity, T_s and T_∞ the average surface and atmospheric temperatures respectively (K), rh the relative humidity (expressed between 0 and 1), $P_{sv}(T_\star)$ (Pa) the saturation vapor pressure at the temperature $T_\star$, and k the average water transfer coefficient (kg.m^{-2}.Pa^{-1}.s^{-1}).

The saturation vapor pressures are classically calculated with empirical relations as the Goff-Gratch equation [30]. However, the ripening temperature is usually between 12 °C and 14 °C. For this low range of temperature, an approximation can be done for saturation vapor pressure values, using a linear regression on the Goff-Gratch equation. The following relation is used:

$$P_{sv}(T_\star) = \beta_1 T_\star + \beta_2 \qquad (18)$$

where β_1 = 102 Pa.K^{-1} and β_2 = −27643 Pa. The relative error (residual standard deviation over value range) is equal to 0.48%.

Direct heat exchange between the cheese and the atmosphere result from convective and radiative fluxes (see Figure 2)

$$\psi_{cr} = h (T_s - T_\infty) + \epsilon \sigma \left(T_s^4 - T_\infty^4 \right) \qquad (19)$$

with h the average convective heat transfer coefficient (W.m^{-2}.K^{-1}), ϵ the product emissivity (dimensionless) and σ the Stefan-Boltzmann constant (W.m^{-2}.K^{-4}). The radiative heat flux relation causes a strong nonlinearity; it can be approximated as following:

$$\epsilon \sigma \left(T_s^4 - T_\infty^4 \right) \simeq 4 \epsilon \overline{T}_\infty^3 (T_s - T_\infty) \qquad (20)$$

where $\overline{T}_\infty$ is the atmospheric temperature mean value. It is then possible to define a global heat transfer coefficient $h^\star = h + 4 \epsilon \sigma \overline{T}_\infty^3$. From [21], we define an empirical relation between h and k for product with cheese shape

$$k = 0.75 \times 10^{-8} h \qquad (21)$$

In addition, the moisture loss induces an heat consumption flux $\psi_w = \lambda \phi_w$ for the evaporation, with λ the water latent vaporization heat (J.kg^{-1}).

High biological activity is observed during the ripening for Camembert-type cheeses with an important mycelial development on the rind. This phenomenon induces a respirative heat production. The generic glucose aerobic respiration equation is

$$\begin{aligned} C_6H_{12}O_6 + \quad & 6O_2 \longrightarrow \\ & 6H_2O + 6CO_2 + 2.816 \times 10^6 \text{J.mol}^{-1} \end{aligned} \qquad (22)$$
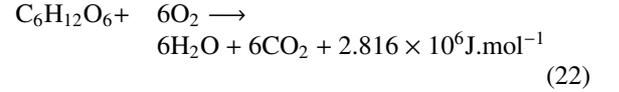
We have with this equation an equimolarity between O_2 and CO_2. During ripening, many substrates are oxidized (lactose, lactate, lipids and proteins), which can induce small differences between O_2 consumption and CO_2 production. This variability is then represented by the average of the gases rates r.

The cheese temperature dynamical model is

$$\frac{dT_s}{dt} = \frac{s}{mC}(-\psi_{cr} - \lambda \phi_w + \alpha \, r) \qquad (23)$$

with m the mass of a cheese, s (m^2) the surface exchange of the cheese, C the specific heat (J.kg^{-1}.K^{-1}) and α the respiration heat (J.mol^{-1}) determined according to (22).

The mass loss dynamic is very slow compared to temperature dynamic, what allows to take T_s at the steady-state. We can thus write

$$T_s = \frac{h^\star T_\infty - \lambda k (a_{ws}\beta_2 - rh (\beta_1 T_\infty + \beta_2)) + \alpha r}{h^\star + \lambda k a_{ws} \beta_1} \qquad (24)$$

and the mass loss rate q_m is defined by

$$\begin{aligned} q_m = \quad & \gamma h^\star (a_{ws} - rh)(\beta_1 T_\infty + \beta_2) \\ & + (\gamma a_{ws}\beta_1 \alpha + w_c) \, r \end{aligned} \qquad (25)$$

with

$$\gamma = \frac{k}{h^\star + \lambda k a_{ws} \beta_1}$$

4.3 Information representation

In this Section, we try to represent the available information faithfully relative to input variables and model parameters.

4.3.1 model parameters

Knowledge about heat respiration α, water latent vaporization heat λ, product emissivity ϵ, Stefan-Boltzmann constant σ and molar mass w_c come from literature (see Table 1).

Surface water activity (a_{ws}) is a key parameter for relation (17). Experimental measurements allows us to assume a_{ws} as constant equal to 0.976.

Due to low airflow velocity inside ripening chamber, available knowledge about the convective heat transfer coefficient h is imprecise and incomplete. Experts consider that heat transfer coefficient is most likely to lie between 3 and 3.2 W.m^{-2}.K^{-4} but they do not exclude values as low as 2.5 and as high as 3.5 W.m^{-2}.K^{-4}. Hence, the knowledge of convective heat transfer coefficient h is represented by means of a trapezoidal possibility distribution of core [3,3.2] and support [2.5,3.5] (see Figure 3). According to
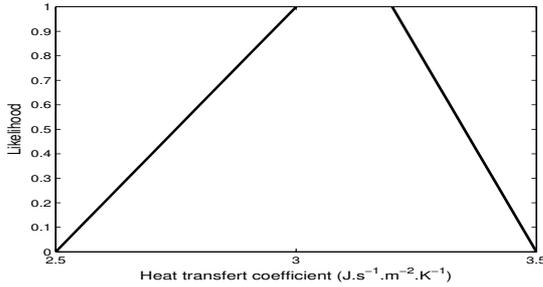
Figure 3: Trapezoidal possibility distribution representing convective heat transfer coefficient h

equation (21), knowledge about the average water transfer coefficient k is also represented by a trapezoidal possibility distribution.

4.3.2 input variables

The mass loss rate (25) is a function of 3 input variables which describe the gas exchanges (r) between cheese and atmosphere and the climatic condition (T_∞, rh). Measurements have not shown significant spatial gradient for O_2 and CO_2 concentrations inside the ripening room. Consequently, the measurements carried out at the position b (see Figure 1) are assumed as representative of gas concentrations close to the cheese. In ripening rooms, as well as cold chambers, due to air condition control, spatial variations of humidity rh and temperature T_∞ are always observed. These gradients are determined by the shape of the
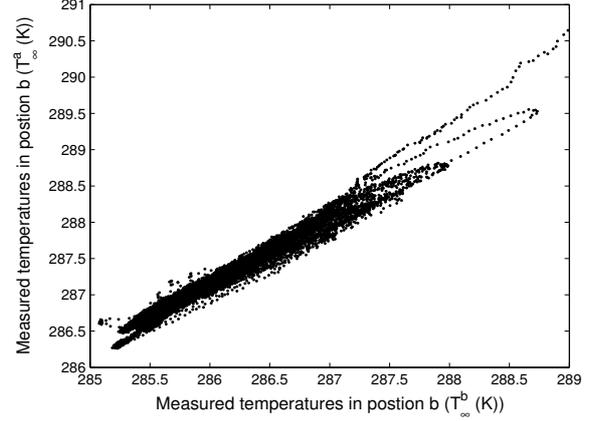
Figure 4: Temperature acquisition in postion a (T_∞^a) vs temperature acquisition in position b (T_∞^b) (see Figure 1).

room and the air regulation device. They are apprehended with detailed measurements and computational fluid dynamic models (*e.g.* see [19]) but these approaches can not be easily performed. We recall that it is inconceivable to install control sensors everywhere inside ripening rooms in order to model the behavior of humidity rh and temperature T_∞ inside chamber. In the present work, the aim is thus to estimate climatic conditions (T_∞, rh) close to cheeses (see Figure 1) from on-line temperature and relative humidity measurements in position b (denoted T_∞^b, rh^b), which is realistic in an industrial context. It is observed a linear relationship (see Figure 4 for temperatures) between climatic conditions (T_∞^a, rh^a) measured by sensors in position a and (T_∞^b, rh^b) measured in position b (see Figure 1, position a & position b). From a linear regression analysis, we obtain:

$$T_\infty^a = 0.91 T_\infty^b + 2.31 \text{ and } rh^a = 1.029 rh^b - 0.064 \quad (26)$$

with residual standard deviations $\sigma_{T_\infty} = 6.6\%$, $\sigma_{rh} = 0.5\%$. Due to low airflow velocity, experts assume that linear relationships remain valid between measured climatic conditions (T_∞^b, rh^b) and those close to by cheeses everywhere inside ripening chamber. However, due to the ill-known spatial variations of humidity and temperature inside ripening room, the linear relationships are tainted with imprecision. According to expert opinions, the imprecision about linear relationships is characterized by the imprecise bias of linear models. That means that temperature T_∞ and relative humidity rh perceived by each cheese can be encoded by:

$$T_\infty = a_{T_\infty} \times T_\infty^b + b_{T_\infty} \text{ and } rh = a_{rh} \times rh^b + b_{rh}$$

where $b_{T_\infty} \in [\underline{b}_{T_\infty}, \overline{b}_{T_\infty}]$ and $b_{rh} \in [\underline{b}_{rh}, \overline{b}_{rh}]$. Finally, by using linear regressions (26) and the empirical knowledge of system by experts, we decided, in the present work, to represent T_∞ (resp. rh) by an imprecise normal distribution

Symbol	Mode of representation
a_{ws} (unit less)	0.976
h (W.m^{-2}.K^{-1})	Trapezoidal possibility distribution support=[2.5,3.5], core=[3,3.2]
k (kg.m^{-2}.Pa^{-1}.s^{-1})	0.75×10^{-8}h
r (unit less)	measures
T_∞ (K)	Imprecise normal distribution $\mathcal{N}(a_{T_\infty} T_\infty^b + b_{T_\infty}, \sigma_{T_\infty})$ $a_{T_\infty} = 0.91$ $b_{T_\infty} \in [2.26, 2.36]$ $\sigma_{T_\infty} = 0.075$
rh (unit less)	Imprecise normal distribution $\mathcal{N}(a_{rh} rh + b_{rh}, \sigma_{rh})$ $a_{rh} = 1.029$ $b_{rh} \in [-0.066, -0.062]$ $\sigma_{rh} = 0.005$
α (J.mol^{-1})	4.693×10^5
λ (J.kg^{-1})	2.47×10^6
ϵ (unit less)	0.91
σ(W.m^{-2}.K^{-4})	5.67×10^{-8}

Table 1: Representation of model parameters & input variables.

$\mathcal{N}(a_{T_\infty} T_\infty^b + b_{T_\infty}, \sigma_{T_\infty})$ (resp. $\mathcal{N}(a_{rh} rh^b + b_{rh}, \sigma_{rh})$) where $(a_{T_\infty}, b_{T_\infty}, \sigma_{T_\infty}) \in \{0.91\} \times [2.31 - 0.5, 2.31 + 0.5] \times \{0.075\}$ (resp. $(a_{rh}, b_{rh}, \sigma_{rh}) \in \{1.029\} \times [-0.064 - 0.02, -0.064 + 0.02] \times \{0.005\}$. Table 1 summarizes modes of representation selected for the different model parameters and input variables.

5 Uncertainty processing

In this Section, we acknowledge the imprecise nature of available information regarding certain model parameters & input variables (see Table 1) and attempt to jointly propagate variability and imprecision in the estimation of cheese mass loss through ripening process. We assume stochastic independence between the group of random sets (T_∞, rh) and the group of possibilistic variables (h, k). Lastly, we assume independence between information sources pertaining to (T_∞, rh). According to the propagation method described in Section 3, the sketch for estimating the probability measure of cheese mass loss through ripening process is the following:

1. For time $t = t_0$.

2. Select a size L of the input sample.

3. We perform a random selection among focal elements by taking into account dependencies described
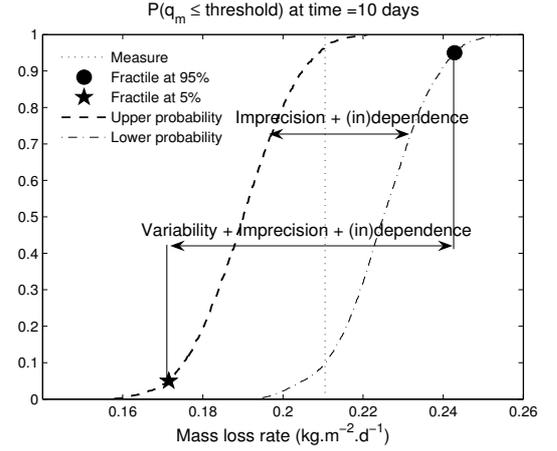
Figure 5: Upper & lower cumulative probabilities of mass loss rate for the tenth day.

previously:

$$\begin{pmatrix} a_{ws} & \pi_{\alpha_1}^h & \pi_{\alpha_1}^k & T_\infty^1(t) & rh^1(t) & r(t) & \alpha & \lambda & \epsilon & \sigma \\ \vdots & \vdots & \vdots & \vdots & \vdots & & \vdots & \vdots & \vdots \\ a_{ws} & \pi_{\alpha_L}^h & \pi_{\alpha_L}^k & T_\infty^L(t) & rh^L(t) & r(t) & \alpha & \lambda & \epsilon & \sigma \end{pmatrix}$$

where, $\forall i = 1, \ldots, L$,

$$T_\infty^i(t) = [a_{T_\infty} T_\infty^b(t) + \underline{b}_{T_\infty} + \sigma_{T_\infty} u_i, a_{T_\infty} T_\infty^b(t) + \overline{b}_{T_\infty} + \sigma_{T_\infty} u_i]$$

$$rh^i(t) = [a_{rh} rh^b(t) + \underline{b}_{rh} + \sigma_{rh} v_i, a_{rh} rh^b(t) + \overline{b}_{rh} + \sigma_{rh} v_i]$$

and $(u_1, \ldots, u_L)$, $(v_1, \ldots, v_L)$ are random sampling from $\mathcal{N}(0, 1)$.

4. Propagate the sample through the model $q_m(t)$, we obtain a random set with focal elements $([\underline{q}_m^i(t), \overline{q}_m^i(t)])_{i=1,\ldots,L}$ defined by:

$$\underline{q}_m^i(t) = \inf_{(h,k,T_\infty,rh) \in \pi_{\alpha_i}^h \times \pi_{\alpha_i}^k \times T_\infty^i(t) \times rh^i(t)}$$

and

$$\overline{q}_m^i(t) = \sup_{(h,k,T_\infty,rh) \in \pi_{\alpha_i}^h \times \pi_{\alpha_i}^k \times T_\infty^i(t) \times rh^i(t)}$$

5. Hence, we can estimate $Bel(q_m(t) \in A)$ by:

$$Bel(q_m(t) \in A) = \frac{1}{L} Card\{i | [\underline{q}_m^i(t), \overline{q}_m^i(t)] \subseteq A\}$$

6. $t = t + \delta t$, return to step 1.

In order to illustrate the impacts of imprecision and variability on mass loss rate, We decided to show, through Figure 5, the upper ($Pl(q_m(10) \le .)$) & lower ($Bel(q_m(10) \le .)$) cumulative distribution functions of it for the tenth day. It also illustrates a comparison with the mass loss rate obtained from online acquisition in position a. The gap between these two distributions is primarily a consequence

of the imprecise nature of available information and, to a lesser extent, of the choice of the dependence in propagation method. According to Figure 5, there is a 5% (resp. 95%) of plausibility (resp. belief) of being lower than 0.172 kg.m^{-2}.d^{-1} (resp. 0.243 kg.m^{-2}.d^{-1}). We can
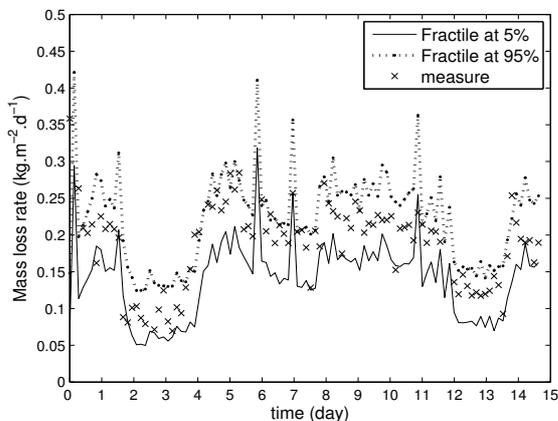
Figure 6: Uncertainty margins of 5% & 95% percentiles pertaining to the mass loss rate through ripening process.

then summarize the uncertainty on mass loss rate for the
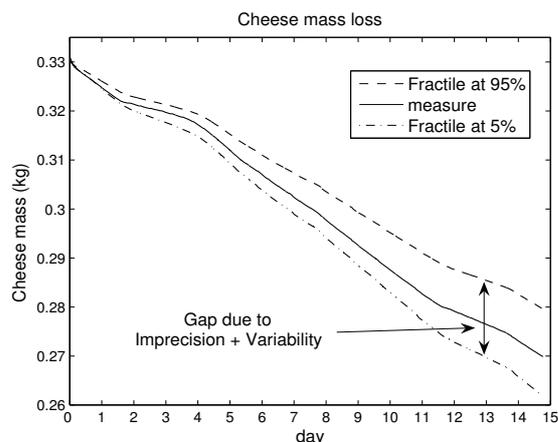
Figure 7: Uncertainty margins of 5% & 95% percentiles pertaining to the cheese mass loss through ripening process.

tenth day by means of interval [0.172 0.243] which can be seen as "confidence interval" containing imprecision. That means, for instance, we are sure at 95% that mass loss rate exceeds 0.172 kg.m^{-2}.d^{-1} for the tenth day. Figure 6 presents uncertainty margins of 5% and 95% percentiles pertaining to the mass loss rate for each time step through ripening process.

After integrate mass loss rate, Figure 7 presents uncertainty margins of 5% and 95% percentiles pertaining to the cheese mass loss for each time step through ripening

process. That means $[e_1^t, e_2^t]$ such that

$$Pl(m_{init} - \int_0^t q_m(u)du \le e_1^t) = 5\%$$

$$Bel(m_{init} - \int_0^t q_m(u)du \le e_2^t) = 95\%$$

where $m_{init} = 0.333kg$. Hence, the probability, at the fifteenth day, of being lower than 0.263 kg is inferior to 5% and the probability of being lower than 0.278 kg is superior to 95%. That means that mass cheese is upper than 0.263 kg and lower than 0.278 kg with a confidence level superior to 90% at the fifteenth day of ripening process. On the one hand, we are sure at 95% that the mass loss of cheese does not exceed 67 g through 15 days of ripening; on the other hand, we are sure at 95% that cheese losses at least 52 g during 15 days.

6 Conclusion

During cheese ripening, a mass loss occurs resulting from heat and mass transfers from cheese to atmosphere. This phenomenon is based on physical laws and biological activity. The state of knowledge to model the process induces uncertainty on some phenomenon and as a consequence on some parameters of it. In this paper, we have quantified uncertainty on the model of cheese ripening mass loss by treating imprecision and variability.

Propagating imprecision on the basis of the results shown, shall help us to improve the control process. It is interesting to notice that a strategy to complete this knowledge can be elaborated as to be able to give a better estimation of the mass loss at the end of the ripening process. For example, considering the large gap between the upper and lower bounds on probability in Figure 5, it is clear that further studies on heat transfer coefficient and climatic conditions would be needed in order to reduce the subjective uncertainty regarding these quantities.

Such a result shows that it is possible to integrate and process mathematically the uncertainty on a complex process such as cheese ripening. Further studies will focus on this last point and moreover on the way to process uncertainty on a more general frame of knowledge integration and dynamic reconstruction.

References

[1] Baudrit, C., Dubois, D. Practical Representation of Incomplete Probabilistic Knowledge. *Comput. Stat. Data Anal.*, 51(1), 86-108, 2006.

[2] Baudrit, C., Couso, I., Dubois, D. Joint Propagation of Probability and Possibility in Risk Analysis: toward a formal framework. *Int. J. of Appro. Reason.*, 45(1), 82-105,

2007.

[3] Baudrit, C., Dubois, D., Guyonnet, D. Joint Propagation and Exploitation of Probabilistic and Possibilistic Information in Risk Assessment Models. *IEEE Trans. on Fuzzy Syst.*, 14(5), 593-608, 2006.

[4] Couso, I., Moral, S., Walley, P. A survey of concepts of independence for imprecise probabilities. *Risk Decision and Policy*, 5, 165-180, 2000.

[5] Davidson, V.J., Brown, R.B., Landman, J.J. Fuzzy control system for peanut roasting. *J. Food Eng.*, 41, 141-146, 1999.

[6] De Cooman, G., Aeyels, D. Supremum-preserving upper probabilities. *Information Sciences*, 118, 173-212, 1999.

[7] Dempster, A.P. Upper and Lower Probabilities Induced by a Multivalued Mapping. *Ann. Math. Stat.*, 38, 325-339, 1967.

[8] Dubois, D., Kerre, E., Mesiar, R, and Prade, H. Fuzzy interval analysis.*Fundamentals of Fuzzy Sets*, D. Dubois, H. Prade, Eds. Boston MA: Kluwer, 483-581, 2000.

[9] Dubois, D., Nguyen, H.T., Prade, H. Possibility theory, probability and fuzzy sets: misunderstandings, bridges and gaps. *Fundamentals of Fuzzy Sets*, Dubois,D. Prade,H., Eds: Kluwer , Boston, Mass, 343-438 , 2000.

[10] Dubois, D., Prade, H. When upper probabilities are possibility measures. *Fuzzy Sets Syst.*, 49, 65-74, 1992.

[11] Ferson, S., Ginzburg, L., Kreinovich, V., Myers, D.M., Sentz, K.Construction Probability Boxes and Dempster-Shafer structures. *Sandia National Laboratories, Technical report SANDD2002-4015*, 2003. URL:www.sandia.gov/epistemic/Reports/SAND2002-4015.pdf.

[12] Ferson, S., Ginzburg, L.R. Different methods are needed to propagate ignorance and variability. *Reliability Engineering and Systems Safety*, 54, 133-144, 1996.

[13] Goodman, I.R., Nguyen, H.T. *Uncertainty Models for Knowledge-Based Systems; A Unified Approach to the Measurement of Uncertainty*, Elsevier Science Inc., New York, NY, 1985.

[14] Helias, A., Mirade, P.S., Corrieu, C. Sensitivity analysis of a simplified cheese ripening mass loss model. Accepted to *10^{t}h Computer Application in Biotechnology*, Cancún, México, 2007.

[15] Ioannou, I., Mauris, G., Trystram, G., Perrot, N. Back-propagation of imprecision in a cheese ripening fuzzy model based on human sensory evaluations. *Fuzzy Sets Syst.*, 157(9), 1179-1187, 2006.

[16] Ioannou, I., Perrot, N., Mauris G., Trystram, G. Building of a control system using fuzzy set theory applied to a browning process, parts 1 and 2, *J. Food Eng.*, 64, 497-514, 2004.

[17] Ioannou, I., Perrot, P., Mauris G., Trystram G. Experimental analysis of sensory measurement imperfection impact for a cheese ripening fuzzy model. *Fuzzy Sets Syst. IFSA 2003*, eds T. Bilgic, B. De Baets, O. Kaynak, Springer, 595-602, 2003.

[18] Kriegler, E., Hermann, H. Utilizing belief functions for the estimation of future climate change. *Int. J. Appro. Reason.*, 39, 185-209, 2005.

[19] Mirade P.-S., Rougier T., Daudin J.-D., Picque D. and Corrieu G. Effect of design of blowing duct on ventilation homogeneity around cheeses in a ripening chamber. *Journal of Food Engineering*, 75(1), 59-70.

[20] Mirade, P.S., Daudin, J.D. Computational fluid dynamics prediction and validation of gas circulation in a cheese-ripening room. *I. Dairy Journal*, 16(8), 920-930, 2006.

[21] Mirade, P.S. and T. Rougier and A. Kondjoyan and J.D. Daudin and D. Picque & G. Corrieu. Caractérisation expérimentale de l'aéraulique d'un hâloir de fromagerie et des changes air-produit. *Lait*, 84, 483-500, 2004.

[22] Leclercq-Perlat, M.N., and F. Buono and D. Lambert and E. Latrille and H.-E. Spinnler and G. Corrieu. Controlled production of Camembert-type cheeses. Part 1: Microbiological and physicochemical evolutions. *J. Dairy Res.*, 35, 346-354, 2004.

[23] Perrot, N., Ioannou, I., Allais, I., Curt, C., Hossenlopp J. & Trystram, G. Fuzzy concepts applied to food product quality control: A review. *Fuzzy Sets Syst.*, 157(9), 1145-1154, 2006.

[24] Perrot, N., Agioux, L., Ioannou, I., Trystram, G., Mauris G. & Corrieu, G. Decision support system design using the operator skill to control cheese ripening - Application of the fuzzy symbolic approach. *J. Food Eng.*, 64, 321-333, 2004.

[25] Petermeier, H., Benning, R., Delgado, A;, Kulozik, U., Hinrichs, J., Becker, T. Hybrid model of the fouling process in tubular heat exchangers for the dairy industry. *J.Food Eng.*, 55, 9-17, 2002.

[26] Picque, D., and M.-N. Leclercq-Perlat and G. Corrieu. Effects of Atmospheric Composition on Respiratory Behavior, Weight Loss, and Appearance of Camembert-Type Cheeses During Chamber Ripening. *J.Dairy Sci.*, 89, 3250-3259, 2006.

[27] Shafer, G. *A Mathematical Theory of Evidence*. Princeton University Press, 1976.

[28] Smets P. and Kennes R. (1994). The transferable belief model. *Artificial Intelligence*, 66, 191-234.

[29] Walley, *P. Statistical Reasoning with Imprecise Probabilities*, Chapman and Hall, 1991.

[30] WMO. General meteorological standards and recommended practices, Appendix A, corrigendum. *World Meteorological Organization Technical Regulations*, Geneva, 49, 2000.